Available online at www.sciencedirect.com
SCIENCE DIRECT
Journal of Sound and Vibration 295 (2006) 884–889
JOURNAL OF SOUND AND VIBRATION
www.elsevier.com/locate/jsvi

A thermo-electro-mechanical coupling study of Csaw motions and an application to the ultrasonic spherical motors by TEM–FEM

W. Zhang*, C.Q. Lou, G.H. Fu, L.X. Yang

Department of Civil Engineering, Zhejiang University, Hangzhou 310027, PR China

Received 2 September 2002; received in revised form 15 March 2005; accepted 27 January 2006
Available online 23 May 2006

Abstract

This paper carries out thermo-electro-mechanical element study of anisotropic and piezoelectric curved surface acoustic waves (Csaw) in uniform materials, and dispersed Csaw of inlaid electrode metals, particularly for a novel type of miniature ultrasonic spherical saw motors. An electro-thermo-mechanical acoustic finite element method is chosen with temperature variation introduced and electric potential condensed, its convergence is verified for mechanical vibration spectrums and piezoelectric surface wave velocities. The coupled acoustic influences of Euler angles and temperature gradients in addition to implanted electrode heights and surface curvatures are evaluated on the piezoelectric surface waves. Numerical results are provided for consistent evaluations, and several conclusions with attained curves are drawn to investigate the electromechanically controlled standing wave drive mechanism.

1. Introduction and background

Constitutive and geometric aspects including the temperature features, the anisotropies of piezoelectric materials and the curvatures of the wave surfaces may tend to concurrently influence the actual working frequencies and velocities of surface acoustic waves. Diversity of vibrations and waves have been widely applied in engineering [1–3]. It is significant to select the proper element methods when analyzing high frequency acoustic wave propagation and relatively low frequency stress wave motion. Recently, new miniature ultrasonic motors start to win much attention, as reported they include linear motors with flat propagating surfaces [4] and spherical torque motors with curved surfaces [5]. These ultrasonic motors can be divided into vibration and surface acoustic wave (saw) types. They possess the particular advantages of low noise and high drive. A diagrammatic of curved surface acoustic waves (Csaw) for a novel ultrasonic spherical motor is depicted in Fig. 1 with top and base circular wave propagation surfaces and inlaid metal electrodes. The electromechanical-controlled wave motion in an opposite direction of θ, pushes forward the ball connected to the rotator/radius along the wave propagation surface of the piezoelectric spherical stator

*Corresponding author. Tel.: +0571 8795 1345; fax: +0571 8795 1358.
E-mail address: zhangwu@civil.zju.edu.cn (W. Zhang).

0022-460X/$ - see front matter © 2006 Elsevier Ltd. All rights reserved.
doi:10.1016/j.jsv.2006.01.058

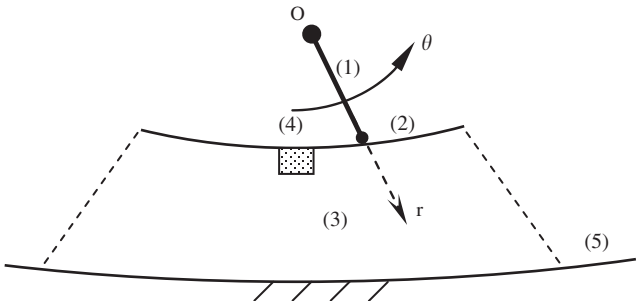

Fig. 1. Schematic part of general anisotropic Csaw: (1) radius, (2) wave propagation surface, (3) piezoelectric spherical crystal substrate, (4) inlaid metal electrode and (5) fixed curved surface base.

substrate, and then the rotator turns in an ultrasonic motor providing torque with regard to the fixed axis at o. This novel piezoelectric wave drive mechanism can make a smaller motor than the conventional electric one. But there is a limit to the wave frequency, otherwise the drive ball will lose contact with the propelling wave surface in an ultrasonic motor, and the prediction accuracies will of course be insufficient. According to the available knowledge, the frequencies and torques of the ultrasonic motors need to be better studied within the frequency range of ultrasonic waves, e.g. less than 100 MHz, lower than most higher frequency saw piezoelectric resonators transmitting signals. In a broader sense, to emphasizing the frequency ranges and operating stabilities becomes of much academic significance and practical importance.

The mentioned coupling analysis is governed and derived by variational principles and will require a finite element method (FEM) with a desirable numerical performance for the Csaw in an ultrasonic device.

This paper is to stress the sound foundations for conducting the different electro-thermo-mechanical (ETM) finite element analyses of the anisotropic Csaw properties in general piezoelectric mixed solids with temperature and inlaid electrodes, in order to discuss the driving wave mechanism of the miniaturized ultrasonic spherical motors with inside and outside surfaces circular. Preliminary and useful results are verified and obtained, respectively, for free flat surface, curved surface and disturbed Csaw motions, and also for beam vibration spectrums.

2. Review of the governing equations for thermo-electro-mechanical element method with static-condensation

To describe the variational principle for the ETM dynamics equations, we first express the kinetic energy in an element level by

$$T = \tfrac{1}{2}\int_v \rho \frac{\partial}{\partial t}\mathbf{U}^{\mathrm{T}} \frac{\partial}{\partial t}\mathbf{U}\,\mathrm{d}v, \tag{1}$$

where v is the element volume; for convenience of notation, $\mathbf{U}$ is defined as displacement vector. The extended potential functional with parameters of temperature change and electric potential is further defined accordingly as

$$\Pi_e(\mathbf{U}, \phi) = \int_v \tfrac{1}{2}\varepsilon^{*\mathrm{T}}\mathbf{C}\varepsilon^{*}\mathrm{d}v, \tag{2}$$

where ϕ is electric potential, ε^{*}stands for generalized strain vector in terms of displacements and potential, and here $\mathbf{C}$ simply denotes the constitutive ETM anisotropic material stiffness matrix,

$$\mathbf{C} = \begin{pmatrix} \mathbf{C}_e & \mathbf{P}_e^{\mathrm{T}} \\ \mathbf{P}_e & \mathbf{D}_e \end{pmatrix} = \mathbf{C}_0 + \mathbf{C}_1\,\Delta T + \mathbf{C}_2\,\Delta T^2 + \mathbf{C}_3\,\Delta T^3, \tag{3}$$

where $\mathbf{C}_e$, $\mathbf{D}_e$ and $\mathbf{P}_e$ are temperature-related mechanical stiffness coefficients, dielectric permittivities and piezoelectric constants of an anisotropic material, respectively. $\Delta T = 0$ means that all the parameters are at room temperature for the electromechanical element method [6].

Without considering much damping in quartz crystals, the electromechanical dynamics equations can be derived by the following modified stationary Hamilton functional which needs boundary conditions, instead of initial conditions, $\delta \int_{t_1}^{t_2} (T - \Pi_e) \mathrm{d}t = 0$, where t = time, T and Π_e are the previously described and expanded kinetic energy and potential energy, respectively.

By variation of this extended Hamilton functional we have the standard generalized governing dynamic equations for electromechanical analysis

$$\mathbf{M}\mathbf{U}'' + \mathbf{K}_{uu}\mathbf{U} + \mathbf{K}_{u\phi}\mathbf{\Phi} = \mathbf{F}, \tag{4}$$

$$\mathbf{K}_{\phi u}\mathbf{U} + \mathbf{K}_{\phi\phi}\mathbf{\Phi} = \mathbf{Q}, \tag{5}$$

where $\mathbf{M}$, $\mathbf{K}_{uu}$, $\mathbf{K}_{u\phi}$ and $\mathbf{K}_{\phi\phi}$ are the mass, mechanical stiffness, piezoelectric coupling and dielectric matrices, while $\mathbf{U}$, $\mathbf{\Phi}$, $\mathbf{F}$ and $\mathbf{Q}$ are the mechanical displacement, electric potential, mechanical force and electric charge vectors, respectively.

For most cases the piezoelectric dynamics equations for vibrations and acoustic waves in arbitrarily shaped hard solids are electro-mechanically coupled, and unfortunately, it usually needs numerical methods like finite and boundary elements to generate a set of governing linear and eigen equations. It is selection and formulation of appropriate solution techniques that matters to carefully balance numerical accuracies and efficiencies, for high frequency acoustic wave propagations and low frequency dynamic stress wave motions, respectively.

If an element method is chosen, an electromechanical structure is first divided into NE elements. For each element we then assume the element field interpolation with vectors of mechanical displacements $\mathbf{U}$ and electric potential $\mathbf{\Phi}$,

$$\begin{Bmatrix} \mathbf{U} \\ \mathbf{\Phi} \end{Bmatrix} = \{ u \quad v \quad w \quad \phi \}^{\mathrm{T}} = \sum_{i=1}^{NE} N_i \{ u \quad v \quad w \quad \phi \}_i^{\mathrm{T}} = \mathbf{N}^* \begin{Bmatrix} \mathbf{q} \\ \boldsymbol{\varphi} \end{Bmatrix}, \tag{6}$$

where N_i $(i = 1, 2, \ldots, \mathrm{NE})$ represent the shape functions of an element with NE nodes, and here again $\mathbf{N}$ implies the element shape function matrix for mechanical displacements only. Specifically, the curved surface waves demand higher order elements, in comparison with flat surface shear ones.

For a generalized plane strain element, the total element strains come from the following differentiation:

$$\begin{aligned} \boldsymbol{\varepsilon}^* &= \{ \varepsilon_x \quad \varepsilon_y \quad \gamma_{yz} \quad \gamma_{zx} \quad \gamma_{xy} \quad \phi_{,x} \quad \phi_{,y} \}^{\mathrm{T}} = \mathbf{D}\{ \mathbf{U} \quad \mathbf{\Phi} \}^{\mathrm{T}} \\ &= \mathrm{diag}(\mathbf{D}_u\mathbf{N}^*, \quad \mathbf{D}_\phi\mathbf{N}^*)\{ \mathbf{q} \quad \varphi \}^{\mathrm{T}} = \mathbf{B}\{ \mathbf{q} \quad \varphi \}^{\mathrm{T}}, \end{aligned} \tag{7}$$

where $\mathbf{D}_u$ and $\mathbf{D}_\phi$ are the differential operators for mechanical and dielectric parts in $\mathbf{D}$, and $\mathbf{N}^*$ stands for the expanded element shape function matrix for electro-mechanical strains. $\mathbf{B} = (\mathbf{B}_u, \mathbf{B}_\phi)$ represents the whole geometric matrix of an element.

When considering the temperature, the element stiffness for ETM analysis is generated in a compact form

$$\mathbf{K} = \begin{pmatrix} \mathbf{K}_{uu} & \mathbf{K}_{u\phi} \\ \mathbf{K}_{u\phi}^T & \mathbf{K}_{\phi\phi} \end{pmatrix} = \int_v \mathbf{B}^{\mathrm{T}}\mathbf{C}\mathbf{B}\,\mathrm{d}v, \tag{8}$$

where the corresponding material matrix, $\mathbf{C}$, is defined in Eq. (3).

The ETM coupling effect in $\mathbf{C}$ and $\mathbf{B}$ in Eqs. (3) and (8), governed by the constitutive generalized plane strain constraint for a piezoelectric crystal, require many more efforts to cope with the material constants and numerical operations. Using the constraint, the required computing capacities are reduced to some extent.

It should be pointed out that different gradient orders of temperature coefficients in Eqs. (3) and (8) will lead to results of difference.

The total element mass matrix for an acoustic element is defined and given by

$$\mathbf{M} = \mathrm{diag}(\mathbf{M}_{uu}, \mathbf{0}) = \left(\int_v \rho \mathbf{N}^{\mathrm{T}} \mathbf{N} \, \mathrm{d}v, 0 \right), \tag{9}$$

where $\mathbf{M}_{uu}$ is the mechanical mass, ρ is its density of a material; specifically for an electrode of Al metal, $\rho = 2699\,\mathrm{kg/cm^2}$, and for quartz crystal, $\rho = 2649\,\mathrm{kg/cm^2}$. Again, here $\mathbf{N}$ denotes the element shape function matrix for consistent mechanical masses.

From Eqs. (1)–(9) we definitely know that the generalized element matrix equations for thermo-electro-acoustic analysis of resonant vibrations and waves are

$$[\mathbf{K}] \begin{Bmatrix} \mathbf{q} \\ \varphi \end{Bmatrix} = \omega^2 [\mathbf{M}] \begin{Bmatrix} \mathbf{q} \\ \varphi \end{Bmatrix}, \tag{10}$$

where ω represents the circular frequency, the stiffness matrix is the expanded one with dielectric part and demands higher order element methods for surface waves, the code can consume a great deal of computer storage and bandwidths in piezoelectric solution that the full-scale piezoelectric saw analysis is still difficult or inaccurate. The element static-condensation of Eq. (10) will avoid numerical scaling in special eigen solutions and can greatly increase computational efficiency. However the rank-deficiency in dielectric matrix has to be resolved.

Without going into details of justifying the computing efficiency and accuracy of the element with perturbation [7] for electromechanical analysis, it is also a normal step here to try and suggest a numerical perturbation to the diagonal terms of the singular dielectric element matrix $\mathbf{K}_{\phi\phi}$ in this ETM analysis of curved surface (disturbed) wave motions, to remove the singularity and fulfill the static-condensation

$$(\mathbf{K}^* - \lambda \mathbf{M}_{uu})\mathbf{q} = \mathbf{0}, \tag{11}$$

where $\mathbf{K}^*$ is the condensed element stiffness matrix here for eigenvalues λ, and is given in the form [2]

$$\mathbf{K}^* = \mathbf{K}_{uu} - \mathbf{K}_{u\phi} \mathbf{K}_{\phi\phi}^{-1} \mathbf{K}_{\phi u} \tag{12}$$

with the following manipulation to execute the inversion after perturbation, i.e., to take

$$\mathbf{K}_{\phi\phi} \cong \mathbf{K}_{\phi\phi} + \Delta \mathbf{K}_{\phi\phi}. \tag{13}$$

It was calculated that this piezoelectric FEM with element static-condensation could make the computing operations plausible by decreasing the storage bandwidths for numerical codes and analyses of multi-periodic piezoelectric saws.

For piezoelectric saws, consider $\Delta \mathbf{K}_{\phi\phi} = \beta \mathbf{I}$, where β is a shift that is problem-dependent with respect to material and wave types, and $\mathbf{I}$ is a unity matrix. Fortunately, β value for Csaw is not large but its range could be wide, the acceptable range value is numerically detected between $\beta = 10^{-16} - 10^{-18}$ for the piezoelectric st-quartz.

3. Verification and application

In the limit as the radius tends to infinite, the curved surface becomes flat with exact solutions. For the time being, it is assumed that the ceramic wear layers on the inlaid metal electrodes are zero in thickness, i.e., the concerned Csaw problem will be confined to the anisotropic piezoelectric spherical substrate solids with a number of isotropic inlaid metal electrodes.

Take two free vibrating beams, the straight one is of $40\,\mu\mathrm{m} \times 2\,\mu\mathrm{m}$ with free boundary conditions in piezoelectric strip resonators, the curved one is shown with radius of $r = 125$ and parallel ends. Two 9-node meshes of 90×5 and 160×8 generalized plane strain elements are used to compute the mechanical vibrating spectrums of the curved beam. The selected mechanical element convergence (rate) is verified for regularly and irregularly meshed beam vibrations as shown in Fig. 2.

For half-wavelength (HW) analysis of Csaw propagation in θ-direction, the element boundary conditions have to be correctly enforced in terms of generalized displacements including potential and tractions for an

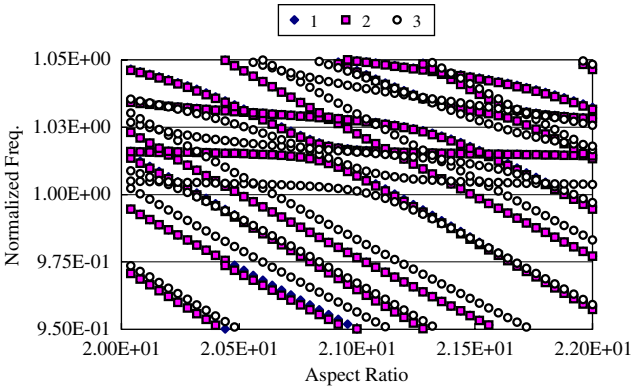

Fig. 2. Converged vibration frequency spectrums of straight and curved st-quartz beams in a strip resonator at room temperature: 1/2-curved beam; and 3 straight beam.

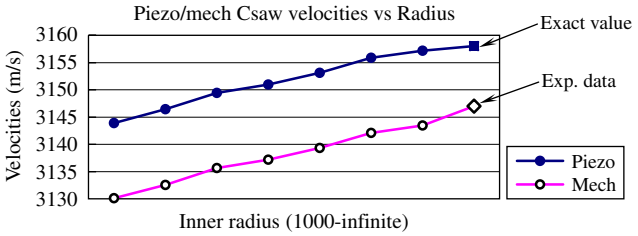

Fig. 3. Curvature effects on st-quartz curved surface acoustic wave velocities.

ultrasonic spherical motor

$$u_x^l(x = x_1) = -u_x^r(x = x_1 + \mathrm{HW}), \quad u_x, u_y, u_z, \phi, \tag{14}$$

$$p_x^l(x = x_1) = -p_x^r(x = x_1 + \mathrm{HW}), \quad p_x, p_y, p_z, \phi_x, \phi_y. \tag{15}$$

Then we verify a flat saw motion close to the surface of the st-quartz solid by choosing the perturbed electromechanical generalized plane finite elements according to the Serendipity and Lagrange types. For a mesh of $8 \times 250 = 2000$, use HW of 5 and the height $h = 100$, the piezoelectric element PQ8 gives the result of 3148.32 close to the mechanical experimental data for saw speed in st-quartz, while PQ9 yields satisfactory solution of 3161.1. A bilinear four-node element should bridge the two in principle, but approximately shares the common properties.

Analyze a half-period st-quartz stator in a spherical ultrasonic motor structure depicted in Fig. 1 by using PQ9. The inner radius varies from 1000 μm (curved surface) to infinitely large (flat surface), the stator thickness $h = 200\,\mu\mathrm{m}$, the curved wave length $= 10\,\mu\mathrm{m}$. The mesh consists of $8 \times 250 = 2000$ nine-node acoustic Lagrange elements. To show how the curved surfaces disturb the Rayleigh saw frequencies and velocities, the mechanical and piezoelectric Csaw velocities vs radii are given and curved in Fig. 3.

It is indicated in Fig. 3 that, with the radius tending to infinite, the piezoelectric Csaw velocity increases without jumps and converges to the exact value of 3158 m/s, and the mechanical Csaw velocity to the laboratory solution of 3149 m/s. As the bending degree increases, the wave velocity will decrease. This quantitative phenomenon turns out to be instrumental to an ultrasonic spherical motor analysis needing a clear constitutive definition and mathematical explanations.

When the temperature changes, inlaid electrode geometries and orientation angles concurrently act on the piezoelectric Csaw motions, the wave or motion speeds could vary in an expected pattern as shown in Table 1 due to the coupling influences or lack of numerical accuracies.

For the time being, we can at least draw the following conclusions after studying the obtained results in Table 1: (1) Temperature increase usually decreases the Csaw speeds in both uniform and embedded materials;

Table 1
Mixed effects on piezoelectric Csaw and Dsaw speeds

Temp. change (°C)	Inlaid electrode thickness	Cut angles	(Thermal) piezoelectric Csaw/Dsaw speeds
0	0.0	40	3163.54
0	0.0	30	3157.78
0	0.0	33(st)	3158.62
0	1.0	33	3202.31
50	1.0	33	3198.10
100	1.0	33	3189.40
0	0.0	30	3157.78
0	0.2	30	3121.53
0	0.4	30	3191.23
0	0.6	30	3188.96

Inlaid electrode width/wave length = 1/8, substrate height = 300.

(2) the thin inlaid metals will make wave speed oscillations in quartz substructures, and (3) the TEM relations for the above two cases turn out to be very complex requiring numerical methods to solve.

4. Discussion and forecast

The ETM coupling element analysis method is successfully designed for a Csaw motor, and assured to be consistent and convergent with the help of exact solutions for free vibrations and flat surface waves. The found relationships together with curves have been partially validated through three techniques, and should be instrumental to the newly arising miniaturized spherical ultrasonic motors for smaller sizes and greater torques with lower noise. If the thickness of the stator substrate is too small, the Bragg condition after Bragg's, may be introduced [8] for leaky wave reflection research, in order to avoid unacceptable interference from the bottom of the piezoelectric stator, except for the inlaid Al electrodes.

To bring the discussion to a close, it is believed that with the obtained knowledge and described methods in this analysis, more potential element simulations of the curved and disturbed saws in ordinary uniform and implanted materials, particularly for an electromechanical saw ultrasonic device together with good operating stabilities, should be finished and validated by the similar analysis process for new piezoelectric anisotropic materials besides quartz crystals.

Acknowledgments

The work partly supported by G.B. CAO High-Tech DF of Zhejiang University.

References

[1] R.D. Mindlin, High frequency vibrations of piezoelectric crystal plates, *International Journal of Solids and Structures* 8 (1972) 895–906.
[2] H. Allik, T.J.R. Hughes, Finite element method for piezoelectric vibrations, *International Journal of Numerical Methods in Engineering* 2 (1970) 151–157.
[3] Z.K. Wang, F. Jin, Influence of curvature on the propagation properties of Rayleigh waves on curved surfaces of arbitrary form, *Acta Mechanica Sinica* (2002).
[4] T. Takano, Y. Tomikawa, Linearly moving ultrasonic motor using a multi-mode vibrator, *Japanese Journal of Applied Physics* 28 (1989) 164–166.
[5] T. Morite, M. Takasak, T. Higuchi, Simulation of surface acoustic wave motor with spherical slider, *IEEE Transactions on Ultrasonics Ferroelectrics and Frequency Control* 46 (4) (1999) 929–934.
[6] W. Zhang, J.C. Tang, Constitutive computational modelling foundation of piezoelectronic microstructures and application to high-frequency microchip DSAW resonators, *Acta Mechanica Sinica* 18 (2) (2002) 170–180 (English Series).
[7] W. Zhang, L.Y. Shi, Y. Chen, D.K. Guo, A new perturbed multivariable finite element method with potential for DSAW computation in plates and layered solids, *Communications in Numerical Methods in Engineering* 18 (12) (2002) 885–898.
[8] G.B. Gustafson, C.H. Wilcox (Eds.), *Analytical and Computational Methods of Advanced Engineering Mathematics*, Springer-Verlag Press, New York, 1998.